

BBB in AD

Gabriel Mateus Bernardo Harrington^{1,2}, Hannah Slevin³, Jimena Monzón-Sandoval^{1,2}, Lara Robinson³, Michal Rokicki⁴, Joanne Morgan⁴, Ngoc-Nga Vinh⁴, Querten Schwarz⁴, Caleb Webber^{1,2}, and Zameel Cader³

¹Cardiff University

²UK Dementia Research Institute

³Oxford University

⁴Centre for Neuropsychiatric Genetics and Genomics, Division of Psychological Medicine and Clinical Neurosciences, School of Medicine, Cardiff University, Cardiff, United Kingdom

Author Note

Gabriel Mateus Bernardo Harrington  <https://orcid.org/0000-0001-6075-3619>

Author roles were classified using the Contributor Role Taxonomy (CRediT; <https://credit.niso.org/>) as follows: Gabriel Mateus Bernardo Harrington: formal analysis, software, writing – original draft, visualization, data curation, conceptualization; Hannah Slevin: method, investigation; Jimena Monzón-Sandoval: writing – original draft, formal analysis, software, visualization, conceptualization; Lara Robinson: method, investigation, writing – original draft; Michal Rokicki: investigation; Joanne Morgan: investigation; Ngoc-Nga Vinh: investigation; Querten Schwarz: investigation; Caleb Webber: writing – original draft, writing – review & editing, project administration, supervision, conceptualization, funding acquisition; Zameel Cader: writing – original draft, writing – review & editing, project administration, supervision, conceptualization, funding acquisition

Correspondence concerning this article should be addressed to Gabriel Mateus Bernardo Harrington, Email: bernardo-harrington@cardiff.ac.uk Caleb Webber

Abstract

The blood brain barrier, it's important, probably in AD even

Keywords: Alzheimer's disease, Blood brain barrier

BBB in AD

0.1 Summary

The interactions between brain parenchymal cells including neurons and glia with brain vascular cells, is crucial for brain homeostasis and is disrupted in Alzheimer's disease (AD) pathogenesis. We developed a method to efficiently isolate parenchymal and vascular nuclei from in post-mortem human brains, achieving over 90% vascular cell enrichment. Using single-nuclei sequencing from 40 samples (20 control and 20 AD cases), we identified risk associations with AD in pericyte and perivascular fibroblast subtypes, as well as in activated microglia. These cells have unique risk signatures linked to amyloid, suggesting a an independent but convergent role in AD risk. Additionally, we discovered EndoMT cells, transitioning from endothelial to mural cells, not previously documented in vascular atlases. This study provides a valuable resource for understanding neurovascular unit composition and dynamics in AD, highlighting potential cellular targets for therapeutic intervention and offering new insights into the cellular interactions associated with amyloid and AD risk.

0.2 Introduction

- Role of BBB in AD
- Prior vascular atlases (Yang), their methods, shortcomings and how our method addresses them

The interface between blood and brain is central to brain function. It serves as both a barrier (the blood-brain-barrier, BBB) [ref] and as a nexus for homeostatic signalling (the neurovascular unit, NVU) [ref]. The BBB protects the brain by preventing harmful substances, such as toxins and pathogens, from entering the central nervous system. It regulates the transport of essential nutrients and aids in the removal of waste products thereby maintaining the brain's stable environment, essential for proper neural function. The concept of the NVU emphasizes the intimate relationship between brain parenchymal and vascular cells for example ensuring sufficient supply of oxygen and glucose to meet the metabolic demands of neurons and glia.([Iadecola, 2017](#))

Alzheimer's disease (AD), the most prevalent type of dementia, is pathologically hallmark by extracellular β -amyloid (A β) deposits, intracellular neurofibrillary tangles (NFTs) and neurodegeneration. The brain's microvasculature, particularly the BBB, plays a crucial role in AD pathophysiology. Endothelial cells (ECs) contribute to the clearance of A β and other toxins, regulate the exclusion of harmful blood proteins, and facilitate immune cell trafficking.(Amersfoort et al., 2022; Daneman & Prat, 2015; Su et al., 2022) Both ECs and pericytes (PCs) are essential for maintaining brain perfusion, endothelial permeability, and immune activation.(Brown et al., 2019; Procter et al., 2021) The BBB's integrity is often compromised in AD, which contributes to disease progression.(Storck et al., 2020; Sweeney et al., 2018) Evidence from imaging, neuropathological studies, and preclinical models indicates chronic tissue hypoxia, impaired cerebral blood flow regulation, and BBB integrity loss in early AD stages, often linked to increased A β levels.(Korte et al., 2020; Nehra et al., 2022)

Knowledge of gene expression levels in brain cell types has transformed the interpretation of AD genetic risk and our understanding of AD molecular pathology (PMIDs). However, despite similar numbers of glia and vascular cells within the brain(Keller et al., 2018), the processes of extracting nuclei from human post-mortem tissue has favoured retrieval of parenchymal nuclei over those of the neurovascular unit (NVU) resulting in a significant underrepresentation of NVU cell types. The first human brain single nuclei atlases examining AD at scale obtained less than a few hundred endothelial cell nuclei as compared to tens of thousands from parenchymal cells, which precluded analyses of the NVU.(Grubman et al., 2019; Mathys et al., 2019) However, the development of extraction approaches focussed on the NVU has recently enabled the study of these cell types. Enrichment approaches have focussed on specifically isolating the neurovasculature from brain samples via mechanical approaches yielding ~50% enrichment of NVU cell type nuclei(Tsartsalis et al., 2024; Yang et al., 2022) which revealed AD-associated impaired angiogenesis and inflammation. Furthermore, both studies highlight potential roles for NVU cell types in mediating the AD genetic risk.

[Paragraph on our work once finished – highlighting having the cell types in the room

delivers better cell type specificity, amyloidosis genetic risk pathways in pericytes, perivascular fibroblasts, activated microglia] plus DEG processes of interest.]

0.3 Results

0.3.1 Isolating the neurovascular unit

Single-cell and single-nuclei RNA sequencing (snRNAseq) has yielded significant insights into health and disease, particularly brain disorders. Traditionally the brain vasculature has been highly challenging to isolate but recent studies have started to examine neurovascular biology through vascular enrichment (Yang et al.; Stergios ..). Whilst a significant advance, the reported vascular nuclei isolation protocols remain relatively inefficient and achieve this enrichment at the expense of parenchymal cells, thereby losing the opportunity to examine whole tissue brain biology. We developed a novel method for the simultaneous isolation of highly pure microvascular nuclei with high-quality parenchymal nuclei from human post-mortem brain tissue in a single procedure.

We identified poor removal of meningeal tissue, poor control of dissection and loss of valuable tissue mass when traditional 4°C dissection of brain tissue was performed using current protocols. We developed a simple unit to enable dissection whilst maintaining tissue temperature at ~-80°C outside of the freezer allowing, careful removal of meninges and other contaminants.

We further created a 3D printed tissue chopper (Fig1A, Supplementary Fig 1) to perform rapid and precise dissection of ultra-cold frozen tissue from solid brain matter into a coarse powder optimal for nuclei isolation, which can then be stored at -80°C until the day of isolation.

Brain vessels are typically lost in standard isolation protocols through under- or over-homogenisation.

We therefore designed 3D printed pestle to allow multiple rounds of large-volume pestle-driven homogenisation combined with low speed centrifugation, enabling efficient release of vessels whilst minimising vessel damage (Fig 1B). This yield vascular pellets and a vessel-free supernatant for parenchymal isolation. Purification of the vascular fraction begins with two multi-layer dextran gradient centrifugation steps to trap contaminants whilst allowing vascular

transfer. The resulting vessel suspension is then filtered through a $100\mu\text{m}$ nylon filter to remove unwanted larger vessels, and vessel capture on $40\mu\text{m}$ PET filters allows depletion of residual contaminating particles. Purified vessels are then transferred onto $20\mu\text{m}$ PET filters for collagenase II digestion of the basement membrane of the vasculature. After the enzyme and released final debris are removed with a wash step, the $20\mu\text{m}$ filter is placed into the 3D printed funnel assembly (supp Fig x) and a hand-held homogeniser is used with a 3D printed flat base pestle to grind the nuclei out of the vessels.

Nuclei after staining with DAPI are isolated using FACS.

The parenchymal supernatant extracted previously is processed to nuclei using standard protocols and similarly FACS isolated.

Extracted and isolated nuclei can then be used with the single-nuclei RNA-seq platform of choice (here 10x Genomics) for transcriptomic analysis.

- Explain isolation (or refer to pre-print if it's ready?)
- The quality/purity of the enrichment
- The cohort details/summary?
- Celltype annotation?
- Compare method directly to Yang atlas paper

0.3.2 *Cohort*

- NOTE: this might get merged into the prior section, but I'll write something for now so it's here. I've already writing some brief stuff in the methods too, not sure how much to add here

We performed single nuclei RNA sequencing on samples from 40 individuals, divided into two groups: 20 AD cases and 20 controls. For each individual, we analysed two fractions: vascular and parenchymal, both sourced from the prefrontal cortex. This resulted in a total of 80 samples (40 vascular and 40 parenchymal).

We obtained 474357 nuclei which was subset to 396103 nuclei after QC (3 donors were also removed in QC) with a median number of genes per nucleus of 2353 post-QC (See Section 0.10.5.2 for QC details). Nuclei were annotated into 12 main cell types which were further subdivided into 44 subtypes based on published markers.([Yang et al., 2022](#))

0.3.3 Differential cell populations

- NOTE: I'll add this here but might be worth moving around to be with section on EndoMT
 - Also may need to update the figure number/panel reference if things move around

As expected, most cell types were preferentially detected in either the vascular or the parenchymal fractions (Figure 1 D) and all cell types were detected among cases and controls (Figure 1 E). However, we observed a reduction in AD cases of proportion of two excitatory neurons subtypes (Ex-Neuro-1 ~75% reduction, $p = 0.001$, FDR = 0.008, Ex-Neuro-5 ~50% reduction, $p = 0.001$, FDR = 0.02) and a subtype of endothelial cells (NA, ~50% reduction, $p = 0.012$, FDR = 0.244; Figure 1 F).

0.3.4 Risk section summary

- TODO:
- Expand on the level 1 T-cell stuff, most of the cell types have t-cell/lymphocyte GO pathways
- Add LD Score risk strip to panel A
- update the PPI network plots - probably need to use cytoscape

0.3.5 Cell type specific Genetic Risk Associations

Having a fuller picture of the parenchymal and vascular fractions of the PFC, we sought to understand which cell types were associated with the genetic risk of AD. To this end, we employed Multi-marker Analysis of Genomic Annotation (MAGMA) along with the latest Genome-Wide Association Study (GWAS) for AD([Bellenguez et al., 2022](#)) and the top 10% cell type specific markers from nuclei of control individuals (see Methods). At the main cell type level and after correcting for multiple testing, our analysis identified microglia, fibroblasts, pericytes, and T-cells associated with AD genetic risk (Figure 2 A).

Further analysis at the subtype level, implicated, in particular, activated microglia (Microglia A), pericyte-2 and perivascular fibroblast 2 (FB-2) with AD genetic risk. While microglia plays a crucial role in the brain immune response and has been implicated before with AD genetic risk, we observed novel associations with pericytes, involved in BBB maintenance and cerebral blood flow regulation, and perivascular fibroblast, essential for the structural integrity of the blood-brain barrier and extracellular matrix composition.

0.3.5.1 Conditional Analysis. We conducted conditional analysis to assess the independence of the risk signals from each cell subtype. The results showed significant enrichment for each of the three cell types even when conditioned on the other two cell types, indicating that the observed signals are unique and not confounded by the other cell types.<NOTE: refer to figure panel of conditional analysis here>

0.3.5.2 Gene Ontology (GO) Enrichment Analysis. To further understand the biological implications of the AD genetic risk genetic associations, we performed Gene Ontology (GO) enrichment analysis on the significant genes identified by MAGMA for each of the aforementioned cell types. The GO analysis revealed several enriched pathways, prominently featuring several amyloid-related processes. The enrichment of genes involved in amyloid precursor protein (APP) processing, amyloid-beta (A β) formation, and amyloid plaque clearance was particularly notable (Figure 2 B). This finding aligns with the well-established role of amyloid pathology in AD. Additionally, for microglia-A and pericyte-2 cell types, significant GO terms related to T-cell and lymphocyte regulation were identified, suggesting an immune regulatory component in AD risk, especially given the significant risk association of T-cells in the main cell type analysis.

0.3.5.3 Protein-Protein Interaction (PPI) Networks. We extracted known protein-protein interaction networks for the significant genes identified in each cell type. The PPI networks all had significantly more interactions than expected by chance. Subsequent Louvain clustering of these networks revealed modules associated with amyloid-related processes (via GO enrichment analysis) across all three cell types (Figure 2 <NOTE: subfig label here>). This

suggests a coordinated risk association involving amyloid processing among microglia-A, pericyte-2, and perivascular-FB-2.

We extracted known protein-protein interaction networks for the significant genes identified in each cell type. The PPI networks all had significantly more interactions than expected by chance. Subsequent Louvain clustering of these networks revealed modules associated with amyloid-related processes (via GO enrichment analysis) across all three cell types (Figure 2D?). This suggests a coordinated risk association involving amyloid processing among microglia-A, pericyte-2, and perivascular-FB-2.

0.3.5.4 Mouse Phenotype Ontology Enrichment Analysis. To further validate our findings, we used the Mouse Phenotype Ontology (MPO) to investigate the functional implications of the significant genes that have one to one orthologs. We subset the database to terms with more than 10 and less than 200 genes and look for more overlap in a term than we would expect by chance. For microglia-A, significant associations were found with the abnormal cell chemotaxis and hematoma terms. Pericyte-2 showed significant associations with amyloidosis and tau protein deposits. However, no significant associations were identified for perivascular-FB-2.

0.3.5.5 Cell-cell communication. We used CellChat to interrogate cell-cell communications and found substantial differences in known ligand-receptor abundances between AD and controls.([Jin, 2024](#)) Signalling pathways showing the greatest overall difference in strength of signalling included Progranulin (GRN), chemokine (CXCL), Tumor necrosis factor-related apoptosis-inducing ligand (TRAIL) and Annexin. These pathways were strongly present in AD and relatively absent in controls. Conversely CALCR and TAC were present in controls and relatively absent in AD. Progranulin, encoded by the gene GRN, is a secreted growth factor which binds to the sortilin receptor (SORT1). Mutations in GRN, which typically lead to reduced progranulin levels (Ward and Mille, 2011) are a cause of fronto-temporal dementia and progranulin is considered a neuroprotective neurotrophic factor. SORT1 polymorphisms are an important AD risk factor and ablation of SORT1 increases progranulin levels. Although not included in the CellChat interactions, progranulin is an antagonist at the TNFa receptor([Tang et](#)

al., 2011) and is anti-inflammatory. Interestingly we find that the dominant source of progranulin appears to be activated microglia, which is strongly present in AD and absent in controls. Many cells from AD samples but not controls appear to be upregulated incoming signalling to progranulin, but in particular oligodendrocytes, vascular cells and T-cells – suggesting that progranulin effects in AD may act on non-neuronal cells to exert trophic and anti-inflammatory effects.

The CXCLs are family of secreted small molecules that bind to G-protein coupled receptors to recruit leukocytes and therefore a critical part of innate immunity. We find an upregulation of chemokine signalling in AD. It is interesting that the perivascular fibroblast population in AD appears to be dominant cell type for outgoing signalling, with receivers being T-cells. TRAIL (also called TNFS10) has been proposed as an important mediator of amyloid-beta induced toxicity.(Cantarella et al., 2003; Cantarella et al., 2014) Its upregulation may suggest its contribution to AD progression. The source appears to be arterial endothelial cells and the responder cells are also endothelial cells which may promote vascular inflammation in AD. In mouse AD models, neutralising TRAIL antibodies was associated with cognitive improvement and reduced inflammation. Annexin A1, which is anti-inflammatory, showed increased signalling in our dataset, and this has previously been shown to be upregulated in Alzheimer's Disease.(Chua et al., 2022) Treatment with recombinant Annexin A1 can improve neurovascular dysfunction, reduce BBB leakage and improve cognitive function.(Ries et al., 2021)

Overall the examination of cell-cell interactions suggests that in AD there is an upregulation of factors involved in immune signalling. In the case progranulin and Annexin A, the expected effect is to counter inflammation whilst chemokines and TRAIL may promote inflammation.

We also specifically examined changes in cell-cell communication between activated microglia, pericyte-2 and perivascular fibroblasts-KAZN. We find communication in pericyte-2 and microglia-A via Transforming Growth Factor β 1 (TGF β 1) as a ligand in pericyte-2 to TGF β Receptor (TGF β R) 1/2 and Activin A Receptor Type 1 (ACVR1) in microglia-A for cases but not

controls, suggesting more activation of microglia by pericytes.<NOTE: refs needed>

- NOTES on cellchat ligand receptor pairs:
 - Pericyte-2 -> Microglia-A (all in cases but not controls):
 - * PTN (Pleiotrophin) -> NCL (Nucleolin) - roles in neuroprotection, neuronal growth and repair - modulating microglia survival/activation?
 - * IL34 -> CSF1R (Colony Stimulating Factor 1 receptor) - similarly likely activating microglia more
 - * BMP6 (Bone morphogenetic protein 6) -> BMPR1A/BMPR2/ACVR1 - again development/activation
 - Microglia-A -> Pericyte-2 (most present in both case and control)
 - * WNT5A -> MCAM - cell adhesion, migration and polarity (BBB integrity?)
 - * TGFB1 -> TGFRB1/2 + ACVR1 (**cases only**) - pericyte activation
 - * SPP1 -> CD44 + ITGAV + ITGB5 + ITGB1 - cell adhesion/migration/survival (BBB/ injury response)
 - * PDGFB -> PDGFRB - pericyte proliferation, survival and recruitment to blood vessels (response to vascular damage?)
 - * LGALS9 -> CD44 - again, adhesion things
 - * GRN -> SORT1 (**cases only**) - inflammatory things
 - * GAS6 -> MERTK + AXL - cell survival (apoptosis?) - anti-inflammatory

0.3.5.6 Interpretation. The identification of these specific cell types and the enrichment of amyloid-related processes underscore the complex interplay between various cellular components in the brain and AD pathology. Microglia-A, pericyte-2, and perivascular-FB-2 may contribute to disease mechanisms through their roles in immune response, vascular integrity, and amyloid processing, respectively. The independence of these signals, as shown by conditional analysis, highlights the unique contributions of each cell type. Additionally, the PPI network analysis suggests a coordinated risk association involving amyloid-related

processes across these cell types. Mouse ontology data further supports these findings, particularly highlighting the roles of microglia-A and pericyte-2 cells in AD-related pathologies.

These findings provide new insights into potential cellular targets for therapeutic intervention in Alzheimer's disease.

0.3.6 Differential Expression Analysis

- ex-neuron 5 - interesting DEGs and sig proportion difference

Using a pseudobulk approach we performed differential gene expression analysis (see Methods) and found the greatest burden of changes on astrocytes, oligodendrocytes and vascular cells – in particular T-pericytes and endothelial cells. Interestingly more genes are upregulated than downregulated in AD in almost all cell types. The cells showing the greatest transcription dysregulation are different to the cell types we found enriched for AD GWAS risk loci. This suggests that the risk loci in these cells may have imparted pathogenic effects earlier in life that are no longer evident. The AD brain instead seems to be dominated by compensatory changes to the disease process or activation of pathways that contribute to ongoing disease progression.

Quiescent astrocytes were the cell type with the most gene changes, with over 600 genes upregulated and approximately 500 genes downregulated. Astrocytes, contact many other cell types including neurons and blood vessels, and have a wide-range of functions from modulating synapse function to being an integral part of the BBB. Using Gene Ontology enrichment analysis we find upregulation of transport pathways and synaptic signalling and support as well as cell adhesion. This is consistent with astrocytes provide trophic support for adjacent neurons amid the ongoing neuro-degeneration. Activated or reactive astrocytes are a feature of many pathological conditions and can have either pro- or anti-inflammatory actions. The majority of genes in reactive astrocytes are upregulated, with pathways involved developmental biological processes. Genes involved in synaptic function are again enriched but unlike quiescent astrocytes, the small number of genes involved (?how many) are downregulated.

Oligodendrocyte precursor cells (OPCs) migrate to a region of injury and differentiate into oligodendrocytes (OLs) that form myelin sheaths for axonal fibres. GSEA of OLs shows

suppression of genes associated with the cilium. The primary cilium is an organelle found in almost all cells and serves a signalling centre to regulate developmental processes. OPCs lose their cilium as they differentiate in OLs. The observed downregulation of cilium genes in OLs in AD may indicate that OLs have recently formed perhaps from OPCs that have reacted to AD associated white matter injury. Another common pathway we detected across DEGs in OL subtypes, was the cholesterol metabolism, which has been previously associated with late AD pathology gene expression changes in OL.([Mathys et al., 2023](#)) The upregulated genes are enriched for immune pathways, suggesting that OLs may be a part of the complex immune environment in AD or responding to immune challenge.

We found one subtype of excitatory neurons exhibiting a large number of differentially expressed genes. Based on the cell identity markers, this excitatory neurons aligned with a deep layer cortical excitatory neurons, that has previously been identified as selectively vulnerable in AD.([Leng et al., 2021](#)) Upregulated genes were enriched for genes involved in response to acetylcholine, a neurotransmitter which is deficient in AD [ref] and which acetylcholinesterase inhibitors used for symptomatic treatment in early AD try to restore [ref]. Further compensatory responses in these neurons is evident in the upregulation of synaptic genes.

In capillary endothelium, a striking upregulated pathway enrichment is the cellular response to insulin. Insulin resistance in AD has been proposed as a key pathogenic mechanism([Talbot et al., 2012](#)), and potentially induced by amyloid. The upregulation of genes involved in insulin signalling may reflect the endothelial response to reducing insulin sensitivity in AD.

T-pericytes, a subtype defined by a previous single cell study of the brain vasculature([Yang et al., 2022](#)) also exhibits a large number of differentially expressed genes. T-pericytes were so called due to higher expression of small molecule transporters but in our study we found that gene set enrichment of upregulated genes in AD highlighted T-cell and leukocyte activation pathways. Notably, SLC4A11 was among the top upregulated genes in T-pericytes and M-pericytes, increased expression of SLC4A11 reduces reactive oxygen

species([Guha et al., 2017](#)), and could be another compensatory mechanism observed in pericytes, or could denote the location of these pericytes, as has been recently proposed as a marker for arteriolar pericytes. In Microglia-A we observed ~60/70 DEGs, similar to other cell types, most of them upregulated, including genes like Translocator Protein (TSPO), which has been previously associated with AD severity. ([Garland et al., 2023](#))

0.4 Discussion

0.5 Acknowledgments

This work is supported by the UK Dementia Research Institute [award number UK DRI-3005] through UK DRI Ltd, principally funded by the Medical Research Council. Part of this work was performed using the computational facilities of the Advance Research Computing @ Cardiff (ARCCA) Division, Cardiff University.

0.6 Author contributions

0.7 Declaration of interests

0.8 Figure titles and legends

0.9 Tables with title and legends

0.10 STAR Methods

Link to info on this here: <https://www.cell.com/star-authors-guide>

And a pdf guide [here](#)

- Plan to make the code available on GitHub and make a docker image with the R environment for all the downstream processing - The seurat object from scflow could be included in this image - This could go on ADDI as well?
- Raw data will go on GEO I guess

0.10.1 Key resources table

0.10.2 Resource availability

0.10.2.1 Lead contact. Further information and requests for resources and reagents should be directed to and will be fulfilled by the lead contact, name here (email here).

0.10.2.2 Materials availability. No unique reagents were generated for this study.

0.10.2.3 Data and code availability.

- All raw data are available in the GEO database under the accession number GEO:
- The Seurat object generated from the scFlow pipeline is included in the Docker image with the R environment used for analysis here:
- All original code has been deposited at Zenodo and is publicly available as of the date of publication. DOIs are listed in the key resources table.

0.10.3 Experimental model and study participant details

0.10.3.1 Post-mortem tissue donors. Post-mortem pre-frontal cortex from 20 controls and 20 AD brain donors were collected from brain bank here under ethics details here. The clinicopathological parameters were collected and summarized in Table S1, including gender, age, diagnosis, APOE status, ethnicity and Braak stage. 3 donors were excluded in QC and of the remaining 37 donors, 23 were female and 14 were male with a median age of 87 (range 48-101). Sex and age were included as a covariates in pseudobulk differential gene expression analysis.

0.10.4 Method details

0.10.4.1 Sample prep/neurovascular unit isolation.

0.10.4.2 RNA sequencing.

0.10.5 Quantification and statistical analysis

0.10.5.1 Data Processing. The raw sequencing data was processed using CellRanger (version 7.1.0, 10X Genomics), which performed initial alignment, filtering, barcode counting, and UMI counting. An updated reference genome (Ensembl version 109 and Gencode version 43 annotations for GRCh38) was generated for use with CellRanger. The resulting gene-barcode

matrices were then further processed using the scFlow pipeline implemented in Nextflow.([Di Tommaso et al., 2017; Khozoe et al., 2021](#))

0.10.5.2 Quality Control. The processed data were read into R (version 4.4.0) using the Seurat package (version 5.1.0).([Hao et al., 2023a; 2024](#)) In addition to the filtering performed by scFlow, cells with low feature/RNA counts were filtered out (between <300 & <7500 for features and >1000 for RNA), and donors with an insufficient number of high-quality cells were excluded from further analysis, resulting in 3 donors (both fractions), and the vascular fraction from 1 addition donor being excluded.

0.10.5.3 Clustering. A standard Seurat workflow was followed including normalisation, finding variable features, scaling and PCA. For the UMAP 35 dimensions and a resolution of 0.6 was used.

0.10.5.4 Cell Type Annotation. Cell types were annotated based on canonical marker genes identified from the literature, Yang et al. ([2022](#)) in particular. The expression levels of these marker genes were used to classify cells into distinct main cell types. These higher level cell types were then subclustered with 20 dimensions and a resolution of 0.4 to identify cell subtypes. This annotation process was validated by comparing the identified cell types to known cell type distributions in similar datasets.

0.10.5.5 Differences in cell proportions. To analyse differences in cell type proportions between case and control groups, we utilized the propeller function from the speckle R package (version 1.4.0) on the vascular and parenchymal fractions separately.([Phipson et al., 2022](#)) This method employs a robust linear modelling framework to test for significant differences in cell type proportions across experimental conditions, while accounting for the compositional nature of the data and potential variability between samples.

0.10.5.6 Pseudobulk differential gene expression. Gene expression data was aggregated by cell type, donor and diagnosis, to create pseudobulk utilising AggregateExpression from Seurat. DESeq2 (version 1.44.0) was employed to run the differential expression, with age and sex as covariates.([Love et al., 2014](#)) This was then used to

perform hypergeometric GO enrichment analysis by filtering to significantly differentially expressed genes (DEGs) (adjusted p-value < 0.05) and running `enrichGO` from `clusterProfiler` (version 4.12.0) with all genes identified in this dataset used as background.([Wu et al., 2021](#))

0.10.5.7 Mammalian Phenotype Ontology enrichment. We use the Jackson Laboratory Mammalian Phenotype Ontology database([Smith & Eppig, 2009](#)) (release 2024-02-07) to test for enrichment of gene lists in phenotypic terms. Given the directed acyclic graph structure of the ontology, we used Simona([Gu, 2023](#)) (version 1.0.10) to annotate child (more specific) terms to their ancestors (more general) terms, creating a deeply annotated set. We further subset the database to terms with more than 10 and less than 200 genes and tested for gene enrichment using an hypergeometric test. We adjusted the p-values using the Benjamini-Hochberg method to account for multiple testing.

0.10.5.8 Cell-cell communication. To investigate cell-cell communication we employed CellChat (version 2.1.2).([Jin, 2024](#)) A CellChat object was created for cases and controls separately using the “Secreted Signalling” ligand-receptor interaction database. A standard CellChat was then followed to identify over expressed genes/ligands and contrast these in cases and controls.

0.10.5.9 Protein-protein interaction networks. We created a combined protein-protein interaction network by combining the following resources: APID([Alonso-López et al., 2019](#)), BIOGRID([Oughtred et al., 2020](#)), BIOPLEX([Hutlin et al., 2021](#)), CORUM([Tsitsiridis et al., 2022](#)), HITPREDICT([López et al., 2015](#)), HuRi([Luck et al., 2020](#)), INTACT([Orchard et al., 2013](#)), MINT([Licata et al., 2011](#)), REACTOME([Gillespie et al., 2021](#)) and only protein physical links from STRING([Szklarczyk et al., 2022](#)). All datasets were mapped to Ensembl Gene ID from either Entrez, Uniprot or Ensembl Protein IDs using org.Hs.eg.db. All duplicated and self-interactions were removed. For any gene set of interest we tested if we observed more interactions than expected by chance. A 10,000 randomizations were used to obtain an empiric p value, reflecting the number of times that equally sized random samples of genes (with similar

degree and gene lenght) had more interactions than our gene set of interest.

0.10.5.10 Disease risk enrichment. To investigate enrichment for disease risk we employed both MAGMA (version 1.10) and LD score (version 1.0.1).([Bulik-Sullivan et al., 2015](#); [Leeuw et al., 2015](#)) We subset to control samples and identified celltype-specific marker genes using FindAllMarkers from the Seurat package.([Hao et al., 2023b](#)) Only genes that are detected in a minimum of 25% of cells in either of the two populations are considered and a minimum log fold change of 0.01 were used. This function was used to apply a Wilcoxon Rank Sum test to compare each cluster against all other clusters identifying differentially expressed gene. From this list of genes, the top ten percent of the total number of genes in the dataset (27459 genes in total) which had the lowest p-values from this test were selected as the celltype specific genes.

The 1000 Genomes Project (Phase 3) was used as a reference in combination with the NCBI37 (GRCh37) genome build as an annotation file.([Auton et al., 2015](#); [Sayers et al., 2022](#)) Genes were annotated with a window 35Kb and 10Kb up/downstream respectively.

0.11 Supplemental information titles and legends

Table S1: Clinical Information. Clinical characteristics of the cohort and samples included in the multi-omics analysis.

Table S2: R packages used

0.12 References

- Alonso-López, D., Campos-Laborie, F. J., Gutiérrez, M. A., Lamourne, L., Calderwood, M. A., Vidal, M., & De Las Rivas, J. (2019). APID database: redefining protein–protein interaction experimental evidences and binary interactomes. *Database*, 2019.
<https://doi.org/10.1093/database/baz005>
- Amersfoort, J., Eelen, G., & Carmeliet, P. (2022). Immunomodulation by endothelial cells — partnering up with the immune system? *Nature Reviews Immunology*, 22(9), 576–588.

<https://doi.org/10.1038/s41577-022-00694-4>

Auton, A., Abecasis, G. R., Altshuler, D. M., Durbin, R. M., Abecasis, G. R., Bentley, D. R., Chakravarti, A., Clark, A. G., Donnelly, P., Eichler, E. E., Flückeck, P., Gabriel, S. B., Gibbs, R. A., Green, E. D., Hurles, M. E., Knoppers, B. M., Korbel, J. O., Lander, E. S., Lee, C., ... National Eye Institute, N. (2015). A global reference for human genetic variation. *Nature*, 526(7571), 68–74. <https://doi.org/10.1038/nature15393>

Bellenguez, C., Küçükali, F., Jansen, I. E., Kleineidam, L., Moreno-Grau, S., Amin, N., Naj, A. C., Campos-Martin, R., Grenier-Boley, B., Andrade, V., Holmans, P. A., Boland, A., Damotte, V., Lee, S. J. van der, Costa, M. R., Kuulasmaa, T., Yang, Q., Rojas, I. de, Bis, J. C., ... Lambert, J.-C. (2022). New insights into the genetic etiology of Alzheimer's disease and related dementias. *Nature Genetics*, 54(4), 412–436. <https://doi.org/10.1038/s41588-022-01024-z>

Brown, L. S., Foster, C. G., Courtney, J.-M., King, N. E., Howells, D. W., & Sutherland, B. A. (2019). Pericytes and neurovascular function in the healthy and diseased brain. *Frontiers in Cellular Neuroscience*, 13. <https://doi.org/10.3389/fncel.2019.00282>

Bulik-Sullivan, B. K., Loh, P.-R., Finucane, H. K., Ripke, S., Yang, J., Patterson, N., Daly, M. J., Price, A. L., & Neale, B. M. (2015). LD Score regression distinguishes confounding from polygenicity in genome-wide association studies. *Nature Genetics*, 47(3), 291–295. <https://doi.org/10.1038/ng.3211>

Cantarella, G., Di Benedetto, G., Puzzo, D., Privitera, L., Loreto, C., Saccone, S., Giunta, S., Palmeri, A., & Bernardini, R. (2014). Neutralization of TNFSF10 ameliorates functional outcome in a murine model of Alzheimer's disease. *Brain*, 138(1), 203–216. <https://doi.org/10.1093/brain/awu318>

Cantarella, G., Uberti, D., Carsana, T., Lombardo, G., Bernardini, R., & Memo, M. (2003). Neutralization of TRAIL death pathway protects human neuronal cell line from β-amyloid toxicity. *Cell Death & Differentiation*, 10(1), 134–141.

<https://doi.org/10.1038/sj.cdd.4401143>

Chua, X. Y., Chong, J. R., Cheng, A. L., Lee, J. H., Ballard, C., Aarsland, D., Francis, P. T., &

- Lai, M. K. P. (2022). Elevation of inactive cleaved annexin A1 in the neocortex is associated with amyloid, inflammatory and apoptotic markers in neurodegenerative dementias. *Neurochemistry International*, 152, 105251. <https://doi.org/10.1016/j.neuint.2021.105251>
- Daneman, R., & Prat, A. (2015). The Blood–Brain Barrier. *Cold Spring Harbor Perspectives in Biology*, 7(1), a020412. <https://doi.org/10.1101/cshperspect.a020412>
- Di Tommaso, P., Chatzou, M., Floden, E. W., Barja, P. P., Palumbo, E., & Notredame, C. (2017). Nextflow enables reproducible computational workflows. *Nature Biotechnology*, 35(4), 316–319. <https://doi.org/10.1038/nbt.3820>
- Garland, E. F., Dennett, O., Lau, L. C., Chatelet, D. S., Bottlaender, M., Nicoll, J. A. R., & Boche, D. (2023). The mitochondrial protein TSPO in Alzheimer’s disease: relation to the severity of AD pathology and the neuroinflammatory environment. *Journal of Neuroinflammation*, 20(1). <https://doi.org/10.1186/s12974-023-02869-9>
- Gillespie, M., Jassal, B., Stephan, R., Milacic, M., Rothfels, K., Senff-Ribeiro, A., Griss, J., Sevilla, C., Matthews, L., Gong, C., Deng, C., Varusai, T., Ragueneau, E., Haider, Y., May, B., Shamovsky, V., Weiser, J., Brunson, T., Sanati, N., ... D’Eustachio, P. (2021). The reactome pathway knowledgebase 2022. *Nucleic Acids Research*, 50(D1), D687–D692. <https://doi.org/10.1093/nar/gkab1028>
- Grubman, A., Chew, G., Ouyang, J. F., Sun, G., Choo, X. Y., McLean, C., Simmons, R. K., Buckberry, S., Vargas-Landin, D. B., Poppe, D., Pflueger, J., Lister, R., Rackham, O. J. L., Petretto, E., & Polo, J. M. (2019). A single-cell atlas of entorhinal cortex from individuals with Alzheimer’s disease reveals cell-type-specific gene expression regulation. *Nature Neuroscience*, 22(12), 2087–2097. <https://doi.org/10.1038/s41593-019-0539-4>
- Gu, Z. (2023). simona:a comprehensive r package for semantic similarity analysis on bio-ontologies. <http://dx.doi.org/10.1101/2023.12.03.569758>
- Guha, S., Chaurasia, S., Ramachandran, C., & Roy, S. (2017). SLC4A11 depletion impairs NRF2 mediated antioxidant signaling and increases reactive oxygen species in human corneal endothelial cells during oxidative stress. *Scientific Reports*, 7(1).

<https://doi.org/10.1038/s41598-017-03654-4>

Hao, Y., Stuart, T., Kowalski, M. H., Choudhary, S., Hoffman, P., Hartman, A., Srivastava, A., Molla, G., Madad, S., Fernandez-Granda, C., & Satija, R. (2023a). *Dictionary learning for integrative, multimodal and scalable single-cell analysis*.

<https://doi.org/10.1038/s41587-023-01767-y>

Hao, Y., Stuart, T., Kowalski, M. H., Choudhary, S., Hoffman, P., Hartman, A., Srivastava, A., Molla, G., Madad, S., Fernandez-Granda, C., & Satija, R. (2023b). *Dictionary learning for integrative, multimodal and scalable single-cell analysis*.

<https://doi.org/10.1038/s41587-023-01767-y>

Hutlin, E. L., Bruckner, R. J., Navarrete-Perea, J., Cannon, J. R., Baltier, K., Gebreab, F., Gygi, M. P., Thorneck, A., Zarraga, G., Tam, S., Szpyt, J., Gassaway, B. M., Panov, A., Parzen, H., Fu, S., Golbazi, A., Maenpaa, E., Stricker, K., Guha Thakurta, S., ... Gygi, S. P. (2021). Dual proteome-scale networks reveal cell-specific remodeling of the human interactome. *Cell*, 184(11), 3022–3040.e28. <https://doi.org/10.1016/j.cell.2021.04.011>

Iadecola, C. (2017). The Neurovascular Unit Coming of Age: A Journey through Neurovascular Coupling in Health and Disease. *Neuron*, 96(1), 17–42.

<https://doi.org/10.1016/j.neuron.2017.07.030>

Jin, S. (2024). *CellChat: Inference and analysis of cell-cell communication from single-cell and spatially resolved transcriptomics data*. <https://github.com/jinworks/CellChat>

Keller, D., Erö, C., & Markram, H. (2018). Cell densities in the mouse brain: A systematic review. *Frontiers in Neuroanatomy*, 12. <https://doi.org/10.3389/fnana.2018.00083>

Khozoie, C., Fancy, N., Marjaneh, M., Murphy, A., Matthews, P., & Skene, N. (2021). *scFlow: A scalable and reproducible analysis pipeline for single-cell RNA sequencing dat*.

<https://doi.org/10.22541/au.162912533.38489960/v2>

Korte, N., Nortley, R., & Attwell, D. (2020). Cerebral blood flow decrease as an early pathological mechanism in Alzheimer's disease. *Acta Neuropathologica*, 140(6), 793–810.

<https://doi.org/10.1007/s00401-020-02215-w>

- Leeuw, C. A. de, Mooij, J. M., Heskes, T., & Posthuma, D. (2015). MAGMA: Generalized Gene-Set Analysis of GWAS Data. *PLOS Computational Biology*, 11(4), e1004219. <https://doi.org/10.1371/journal.pcbi.1004219>
- Leng, K., Li, E., Eser, R., Piergies, A., Sit, R., Tan, M., Neff, N., Li, S. H., Rodriguez, R. D., Suemoto, C. K., Leite, R. E. P., Ehrenberg, A. J., Pasqualucci, C. A., Seeley, W. W., Spina, S., Heinsen, H., Grinberg, L. T., & Kampmann, M. (2021). Molecular characterization of selectively vulnerable neurons in Alzheimer's disease. *Nature Neuroscience*, 24(2), 276–287. <https://doi.org/10.1038/s41593-020-00764-7>
- Licata, L., Briganti, L., Peluso, D., Perfetto, L., Iannuccelli, M., Galeota, E., Sacco, F., Palma, A., Nardozza, A. P., Santonico, E., Castagnoli, L., & Cesareni, G. (2011). MINT, the molecular interaction database: 2012 update. *Nucleic Acids Research*, 40(D1), D857–D861. <https://doi.org/10.1093/nar/gkr930>
- López, Y., Nakai, K., & Patil, A. (2015). HitPredict version 4: comprehensive reliability scoring of physical protein–protein interactions from more than 100 species. *Database*, 2015, bav117. <https://doi.org/10.1093/database/bav117>
- Love, M. I., Huber, W., & Anders, S. (2014). *Moderated estimation of fold change and dispersion for RNA-seq data with DESeq2*. 15, 550. <https://doi.org/10.1186/s13059-014-0550-8>
- Luck, K., Kim, D.-K., Lambourne, L., Spirohn, K., Begg, B. E., Bian, W., Brignall, R., Cafarelli, T., Campos-Laborie, F. J., Charlotteaux, B., Choi, D., Coté, A. G., Daley, M., Deimling, S., Desbuleux, A., Dricot, A., Gebbia, M., Hardy, M. F., Kishore, N., … Calderwood, M. A. (2020). A reference map of the human binary protein interactome. *Nature*, 580(7803), 402–408. <https://doi.org/10.1038/s41586-020-2188-x>
- Mathys, H., Davila-Velderrain, J., Peng, Z., Gao, F., Mohammadi, S., Young, J. Z., Menon, M., He, L., Abdurrob, F., Jiang, X., Martorell, A. J., Ransohoff, R. M., Hafler, B. P., Bennett, D. A., Kellis, M., & Tsai, L.-H. (2019). Single-cell transcriptomic analysis of Alzheimer's disease. *Nature*, 570(7761), 332–337. <https://doi.org/10.1038/s41586-019-1195-2>
- Mathys, H., Peng, Z., Boix, C. A., Victor, M. B., Leary, N., Babu, S., Abdelhady, G., Jiang, X.,

- Ng, A. P., Ghafari, K., Kunisky, A. K., Mantero, J., Galani, K., Lohia, V. N., Fortier, G. E., Lotfi, Y., Ivey, J., Brown, H. P., Patel, P. R., ... Tsai, L.-H. (2023). Single-cell atlas reveals correlates of high cognitive function, dementia, and resilience to Alzheimer's disease pathology. *Cell*, 186(20), 4365–4385.e27. <https://doi.org/10.1016/j.cell.2023.08.039>
- Nehra, G., Bauer, B., & Hartz, A. M. S. (2022). Blood-brain barrier leakage in Alzheimer's disease: From discovery to clinical relevance. *Pharmacology & Therapeutics*, 234, 108119. <https://doi.org/10.1016/j.pharmthera.2022.108119>
- Orchard, S., Ammari, M., Aranda, B., Breuza, L., Briganti, L., Broackes-Carter, F., Campbell, N. H., Chavali, G., Chen, C., del-Toro, N., Duesbury, M., Dumousseau, M., Galeota, E., Hinz, U., Iannuccelli, M., Jagannathan, S., Jimenez, R., Khadake, J., Lagreid, A., ... Hermjakob, H. (2013). The MIntAct project—IntAct as a common curation platform for 11 molecular interaction databases. *Nucleic Acids Research*, 42(D1), D358–D363. <https://doi.org/10.1093/nar/gkt1115>
- Oughtred, R., Rust, J., Chang, C., Breitkreutz, B.-J., Stark, C., Willems, A., Boucher, L., Leung, G., Kolas, N., Zhang, F., Dolma, S., Coulombe-Huntington, J., Chatr-aryamontri, A., Dolinski, K., & Tyers, M. (2020). The BioGRID database: A comprehensive biomedical resource of curated protein, genetic, and chemical interactions. *Protein Science*, 30(1), 187–200. <https://doi.org/10.1002/pro.3978>
- Phipson, B., Sim, C. B., Porrello, E. R., Hewitt, A. W., Powell, J., & Oshlack, A. (2022). *Propeller: Testing for differences in cell type proportions in single cell data.* 38, –6. <https://doi.org/10.1093/bioinformatics/btac582>
- Procter, T. V., Williams, A., & Montagne, A. (2021). Interplay between Brain Pericytes and Endothelial Cells in Dementia. *The American Journal of Pathology*, 191(11), 1917–1931. <https://doi.org/10.1016/j.ajpath.2021.07.003>
- R Core Team. (2024). *R: A language and environment for statistical computing*. <https://www.R-project.org/>
- Ries, M., Watts, H., Mota, B. C., Lopez, M. Y., Donat, C. K., Baxan, N., Pickering, J. A., Chau, T.

- W., Semmler, A., Gurung, B., Aleksynas, R., Abelleira-Hervas, L., Iqbal, S. J., Romero-Molina, C., Hernandez-Mir, G., d'Amati, A., Reutelingsperger, C., Goldfinger, M. H., Gentleman, S. M., ... Sastre, M. (2021). Annexin A1 restores cerebrovascular integrity concomitant with reduced amyloid- β and tau pathology. *Brain*, 144(5), 1526–1541.
<https://doi.org/10.1093/brain/awab050>
- Sayers, E. W., Bolton, E. E., Brister, J. R., Canese, K., Chan, J., Comeau, D. C., Connor, R., Funk, K., Kelly, C., Kim, S., Madej, T., Marchler-Bauer, A., Lanczycki, C., Lathrop, S., Lu, Z., Thibaud-Nissen, F., Murphy, T., Phan, L., Skripchenko, Y., ... Sherry, S. T. (2022). Database resources of the national center for biotechnology information. *Nucleic Acids Research*, 50(D1), D20–D26. <https://doi.org/10.1093/nar/gkab1112>
- Smith, C. L., & Eppig, J. T. (2009). The mammalian phenotype ontology: enabling robust annotation and comparative analysis. *WIREs Systems Biology and Medicine*, 1(3), 390–399.
<https://doi.org/10.1002/wsbm.44>
- Storck, S. E., Hartz, A. M. S., & Pietrzik, C. U. (2020). *The blood-brain barrier in alzheimer's disease* (pp. 247–266). Springer International Publishing.
https://doi.org/10.1007/164_2020_418
- Su, Q., Guo, J.-H., Zhang, Y.-L., Wang, J., & Zhang, Z.-N. (2022). The relationship between amyloid-beta and brain capillary endothelial cells in Alzheimer's disease. *Neural Regeneration Research*, 17(11), 2355. <https://doi.org/10.4103/1673-5374.335829>
- Sweeney, M. D., Sagare, A. P., & Zlokovic, B. V. (2018). Blood–brain barrier breakdown in Alzheimer disease and other neurodegenerative disorders. *Nature Reviews Neurology*, 14(3), 133–150. <https://doi.org/10.1038/nrneurol.2017.188>
- Szklarczyk, D., Kirsch, R., Koutrouli, M., Nastou, K., Mehryary, F., Hachilif, R., Gable, A. L., Fang, T., Doncheva, N., Pyysalo, S., Bork, P., Jensen, L., & von Mering, C. (2022). The STRING database in 2023: protein–protein association networks and functional enrichment analyses for any sequenced genome of interest. *Nucleic Acids Research*, 51(D1), D638–D646.
<https://doi.org/10.1093/nar/gkac1000>

Talbot, K., Wang, H.-Y., Kazi, H., Han, L.-Y., Bakshi, K. P., Stucky, A., Fuino, R. L., Kawaguchi, K. R., Samoyedny, A. J., Wilson, R. S., Arvanitakis, Z., Schneider, J. A., Wolf, B. A., Bennett, D. A., Trojanowski, J. Q., & Arnold, S. E. (2012). Demonstrated brain insulin resistance in Alzheimer's disease patients is associated with IGF-1 resistance, IRS-1 dysregulation, and cognitive decline. *The Journal of Clinical Investigation*, 122(4), 1316–1338.

<https://doi.org/10.1172/JCI59903>

Tang, W., Lu, Y., Tian, Q.-Y., Zhang, Y., Guo, F.-J., Liu, G.-Y., Syed, N. M., Lai, Y., Lin, E. A., Kong, L., Su, J., Yin, F., Ding, A.-H., Zanin-Zhorov, A., Dustin, M. L., Tao, J., Craft, J., Yin, Z., Feng, J. Q., ... Liu, C. (2011). The Growth Factor Progranulin Binds to TNF Receptors and Is Therapeutic Against Inflammatory Arthritis in Mice. *Science*, 332(6028), 478–484.

<https://doi.org/10.1126/science.1199214>

Tsartsalis, S., Slevin, H., Fancy, N., Wessely, F., Smith, A. M., Willumsen, N., Cheung, T. K. D., Rokicki, M. J., Chau, V., Ifie, E., Khoozoe, C., Ansorge, O., Yang, X., Jenkyns, M. H., Davey, K., McGarry, A., Muirhead, R. C. J., Debette, S., Jackson, J. S., ... Matthews, P. M. (2024). A single nuclear transcriptomic characterisation of mechanisms responsible for impaired angiogenesis and blood-brain barrier function in Alzheimer's disease. *Nature Communications*, 15(1). <https://doi.org/10.1038/s41467-024-46630-z>

Tsitsirisidis, G., Steinkamp, R., Giurgiu, M., Brauner, B., Fobo, G., Frishman, G., Montrone, C., & Ruepp, A. (2022). CORUM: the comprehensive resource of mammalian protein complexes–2022. *Nucleic Acids Research*, 51(D1), D539–D545.

<https://doi.org/10.1093/nar/gkac1015>

Wu, T., Hu, E., Xu, S., Chen, M., Guo, P., Dai, Z., Feng, T., Zhou, L., Tang, W., Zhan, L., Fu, xiaochong, Liu, S., Bo, X., & Yu, G. (2021). *clusterProfiler 4.0: A universal enrichment tool for interpreting omics data*. 2, 100141. <https://doi.org/10.1016/j.xinn.2021.100141>

Yang, A. C., Vest, R. T., Kern, F., Lee, D. P., Agam, M., Maat, C. A., Losada, P. M., Chen, M. B., Schaum, N., Khoury, N., Toland, A., Calcuttawala, K., Shin, H., Pálovics, R., Shin, A., Wang, E. Y., Luo, J., Gate, D., Schulz-Schaeffer, W. J., ... Wyss-Coray, T. (2022). A human brain

vascular atlas reveals diverse mediators of Alzheimer's risk. *Nature*, 603(7903), 885–892.

<https://doi.org/10.1038/s41586-021-04369-3>

Table 1*Key resources table*

group	REAGENT or RESOURCE	SOURCE	IDENTIFIER
Critical commercial assays	10X Genomics Chromium Single Cell 3' Reagent Kits	10X Genomics	PN- 1820
Deposited data	Raw and analysed data	This paper	GEO: https://www.ncbi.nlm.nih.gov/geo/
Software and algorithms	Cellranger v7.1.0	10X Genomics	https://www.10xgenomics.com/software
Software and algorithms	Nextflow v23.04.1.5866	https://doi.org/10.1038/nbt.1820	//www.nextflow.io/
Software and algorithms	scFlow pipeline v0.7.2	https://doi.org/10.22541/au.1629125138489960/nf-core-scflow/tree/dev-nf	
Software and algorithms	R v4.4.1	R Foundation for Statistical Computing	https://www.R-project.org/
Software and algorithms	Seurat v5.1.0	https://doi.org/10.1038/s41582-023-01767-y	1820
Software and algorithms	Data analysis code	This paper	doi for code goes here

donor_id	sex	age	diagnosis	braak_stage	cerebral_hemisphere	brain_weight	diagnosis_details	apoe_status
NP011/20194	Control	6.04	White	1386	Low level AD Braak II, (Euro-pean)		Abnormal deposition of pTDP-43 in medial temporal lobe	2/4
NP041/20197	Case V	5.57	Black	1034	AD, LATE Caribbean			3/4
NP067/20181	Case VI	6.43	unknown	1172	AD, LBD, CVD, Hippocampal sclerosis			4/4
NP076/20195	Case V	5.94	unknown	934	AD			3/4
NP032/20186	Control III	5.62	unknown	1330	Abnormal deposition of tau protein			2/3
NP150/20195	Control II	5.17	unknown	1317	Normal aged brain			3/3
NP077/20182	Control II	5.90	unknown	1400	Normal aged control, low level AD change			3/4
NP090/M7 70	Control II	NA	NA	NA	Aged brain Braak II			3/3
NP102/M7 81	Control II	NA	NA	NA	Normal aged Brain Braak II			3/3
NP093/M3 90	Case V	NA	NA	NA	Alzheimer's disease, Braak V, CVD			3/3
NP018/M4 85	Case VI	NA	NA	NA	AD Braak VI			3/4
NP406/M6 81	Case VI	NA	NA	NA	AD Braak VI			2/4
NP096/M3 92	Control II	NA	NA	NA	Normal aged brain Braak II			3/3
NP127/M4 89	Case IV	NA	NA	NA	AD Braak IV			4/4
NP080/M5 71	Control I	NA	NA	NA	Normal aged brain Braak I			3/3
NP054/M7 73	Case VI	NA	NA	NA	AD Braak VI			3/4
NP109/M7 77	Control I	NA	NA	NA	Normal aged brain Braak I			3/3
NP048/M9 71	Control I	NA	NA	NA	Aged brain Braak I			3/3

donor_id	sex	age	diagnosis	braak_stage	beta_tangle	tau_cerebral	tau_mimic	brain_weight	diagnosis_details	apoe_status
NP011	M	49	Control	III	NA	NA	NA	Normal aged brain .	Braak III	3/3
NP160	M	83	Case	IV	NA	NA	NA	AD Braak IV, CVD		3/4
NP024	M	74	Control	II	NA	NA	NA	Control with low level AD	Braak II	3/3
NP092	M	98	Case	IV	NA	NA	NA	AD, LATE, CVD	Braak IV	3/4
NP103	M	48	Control	NA	NA	NA	NA	Control		3/3
NP037	M	81	Case	V	NA	NA	NA	AD, CVD	Braak V	3/4
NP016	F	89	Control	II	5.67	unknown	1366	Aged brain, CVD		3/3
NP163	M	89	Case	IV	NA	NA	NA	AD Braak IV, CVD		3/4
NP034	F	87	Case	VI	5.95	unknown	1060	AD		2/4
NP008	F	87	Control	II	6.86	unknown	1101	Normal aged brain		3/3
NP002	M	98	Case	VI	5.63	unknown	1151	AD, CVD		4/4
NP070	M	95	Control	II	6.03	unknown	1367	Control with low level AD		3/3
								change Braak II		
NP128	M	87	Control	I	6.10	unknown	1368	Control, CVD		3/3
NP080	F	89	Case	V	6.67	unknown	1101	AD, LBD, CVD		3/3
NP018	M	97	Case	V	5.93	unknown	1154	AD Braak V		3/4
NP142	M	85	Case	VI	6.22	unknown	1372	AD Braak VI		3/3
NP058	M	89	Control	II	5.58	unknown	1141	Low level AD		3/3
NP177	F	90	Case	V	5.58	unknown	1153	AD, LBD		3/3
NP063	F	89	Control	II	5.69	White	1280	Aged brain (Euro-pean)	Low level AD	3/3

package	loaded	version	source
AnnotationDbi	1.66.0		Bioconductor 3.19 (R 4.4.0)
AnnotationFilter	1.28.0		Bioconductor 3.19 (R 4.4.0)
AnnotationHub	3.12.0		Bioconductor 3.19 (R 4.4.0)
BSgenome	1.72.0		Bioconductor 3.19 (R 4.4.0)
BSgenome.Hsapiens.1000g	0.99.1		Bioconductor
BSgenome.Hsapiens.NCBI.GRC008			Bioconductor
Biobase	2.64.0		Bioconductor 3.19 (R 4.4.0)
BiocFileCache	2.12.0		Bioconductor 3.19 (R 4.4.0)
BiocGenerics	0.50.0		Bioconductor 3.19 (R 4.4.0)
BiocIO	1.14.0		Bioconductor 3.19 (R 4.4.0)
BiocManager	1.30.25		RSPM (R 4.4.1)
BiocNeighbors	1.22.0		Bioconductor 3.19 (R 4.4.0)
BiocParallel	1.38.0		Bioconductor 3.19 (R 4.4.0)
BiocSingular	1.20.0		Bioconductor 3.19 (R 4.4.0)
BiocVersion	3.19.1		Bioconductor 3.19 (R 4.4.0)
Biostrings	2.72.1		Bioconductor 3.19 (R 4.4.1)
CellChat	2.1.2		Github (jinworks/- CellChat@b05405af0f4f2cac99f2211e888d42de4c5a9d59)
ComplexHeatmap	2.20.0		Bioconductor 3.19 (R 4.4.0)
DBI	1.2.3		RSPM (R 4.4.1)
DESeq2	1.44.0		Bioconductor 3.19 (R 4.4.0)
DEoptimR	1.1-3		CRAN (R 4.4.0)
DOSE	3.30.5		Bioconductor 3.19 (R 4.4.1)
DT	0.33		CRAN (R 4.4.0)
DelayedArray	0.30.1		Bioconductor 3.19 (R 4.4.0)

package	loaded	version	source
DelayedMatrixStats	1.26.0		Bioconductor 3.19 (R 4.4.0)
DirichletReg	0.7-1		RSPM (R 4.4.0)
DoubletFinder	2.0.4		Github (chris-mcginnis-ucsf/DoubletFinder@03e9f37f891ef76a23cc55ea69f940c536ae8f9f)
DropletUtils	1.24.0		Bioconductor 3.19 (R 4.4.0)
EWCE	1.12.0		Bioconductor 3.19 (R 4.4.0)
EnsDb.Hsapiens.v79	2.99.0		Bioconductor
ExperimentHub	2.12.0		Bioconductor 3.19 (R 4.4.0)
FNN	1.1.4.1		RSPM (R 4.4.1)
Formula	1.2-5		RSPM (R 4.4.0)
GEOquery	2.72.0		Bioconductor 3.19 (R 4.4.0)
GO.db	3.19.1		Bioconductor
GOSemSim	2.30.2		Bioconductor 3.19 (R 4.4.1)
GenomeInfoDb	1.40.1		Bioconductor 3.19 (R 4.4.1)
GenomeInfoDbData	1.2.12		Bioconductor
GenomicAlignments	1.40.0		Bioconductor 3.19 (R 4.4.0)
GenomicFeatures	1.56.0		Bioconductor 3.19 (R 4.4.0)
GenomicFiles	1.40.0		Bioconductor 3.19 (R 4.4.0)
GenomicRanges	1.56.2		Bioconductor 3.19 (R 4.4.1)
GetoptLong	1.0.5		CRAN (R 4.4.0)
GlobalOptions	0.1.2		CRAN (R 4.4.0)
HDF5Array	1.32.1		Bioconductor 3.19 (R 4.4.1)
HGNHelper	0.8.14		RSPM (R 4.4.0)
IRanges	2.38.1		Bioconductor 3.19 (R 4.4.1)
KEGGREST	1.44.1		Bioconductor 3.19 (R 4.4.1)

package	loaded	version	source
KEGGgraph		1.64.0	Bioconductor 3.19 (R 4.4.0)
KernSmooth		2.23-26	CRAN (R 4.4.2)
MASS		7.3-64	CRAN (R 4.4.2)
MAST		1.30.0	Bioconductor 3.19 (R 4.4.0)
Matrix		1.7-2	CRAN (R 4.4.2)
MatrixGenerics		1.16.0	Bioconductor 3.19 (R 4.4.0)
MungeSumstats		1.12.2	Bioconductor 3.19 (R 4.4.1)
NLP		0.3-1	CRAN (R 4.4.2)
NMF		0.28	RSPM (R 4.4.1)
PCAtools		2.16.0	Bioconductor 3.19 (R 4.4.0)
Polychrome		1.5.1	CRAN (R 4.4.0)
ProtGenerics		1.36.0	Bioconductor 3.19 (R 4.4.0)
R.methodsS3		1.8.2	CRAN (R 4.4.0)
R.oo		1.27.0	RSPM (R 4.4.2)
R.utils		2.12.3	CRAN (R 4.4.0)
R6		2.5.1	CRAN (R 4.4.0)
RANN		2.6.2	RSPM (R 4.4.1)
RApiSerialize		0.1.4	RSPM (R 4.4.1)
RColorBrewer		1.1-3	CRAN (R 4.4.0)
RCurl		1.98-1.16	RSPM (R 4.4.1)
RNOmni		1.0.1.2	RSPM (R 4.4.0)
ROCR		1.0-11	CRAN (R 4.4.0)
RSQLite		2.3.7	RSPM (R 4.4.0)
RSpectra		0.16-2	RSPM (R 4.4.1)
Rcpp		1.0.13-1	RSPM (R 4.4.2)

package	loaded	version	source
RcppAnnoy	0.0.22	CRAN (R 4.4.0)	
RcppHNSW	0.6.0	CRAN (R 4.4.0)	
RcppParallel	5.1.9	CRAN (R 4.4.1)	
ResidualMatrix	1.14.1	Bioconductor 3.19 (R 4.4.1)	
Rgraphviz	2.48.0	Bioconductor 3.19 (R 4.4.0)	
Rhdf5lib	1.26.0	Bioconductor 3.19 (R 4.4.0)	
Rsamtools	2.20.0	Bioconductor 3.19 (R 4.4.0)	
Rtsne	0.17	CRAN (R 4.4.0)	
S4Arrays	1.4.1	Bioconductor 3.19 (R 4.4.1)	
S4Vectors	0.42.1	Bioconductor 3.19 (R 4.4.1)	
SC3	1.32.0	Bioconductor 3.19 (R 4.4.0)	
SNPLocs.Hsapiens.dbSNP13599RCCh37			Bioconductor
SNPLocs.Hsapiens.dbSNP13599RCCh38			Bioconductor
ScaledMatrix	1.12.0		Bioconductor 3.19 (R 4.4.0)
Seurat	5.1.0		RSPM (R 4.4.0)
SeuratObject	5.0.2		RSPM (R 4.4.2)
SeuratWrappers	0.3.5		Github (satijalab/seurat-wrappers@8d46d6c47c089e193fe5c02a8c23970715918aa9)
SingleCellExperiment	1.26.0		Bioconductor 3.19 (R 4.4.0)
SnowballC	0.7.1		CRAN (R 4.4.0)
SparseArray	1.4.8		Bioconductor 3.19 (R 4.4.1)
SparseM	1.84-2		RSPM (R 4.4.1)
SummarizedExperiment	1.34.0		Bioconductor 3.19 (R 4.4.0)
UCSC.utils	1.0.0		Bioconductor 3.19 (R 4.4.0)
UpSetR	1.4.0		RSPM (R 4.4.0)

package	loaded	version	source
VariantAnnotation	1.50.0		Bioconductor 3.19 (R 4.4.0)
WebGestaltR	0.4.6		RSPM (R 4.4.0)
WriteXLS	6.7.0		RSPM (R 4.4.1)
XML	3.99-0.17		RSPM (R 4.4.1)
XVector	0.44.0		Bioconductor 3.19 (R 4.4.0)
abind	1.4-8		RSPM (R 4.4.1)
alabaster.base	1.4.2		Bioconductor 3.19 (R 4.4.1)
alabaster.matrix	1.4.2		Bioconductor 3.19 (R 4.4.1)
alabaster.ranges	1.4.2		Bioconductor 3.19 (R 4.4.1)
alabaster.sce	1.4.0		Bioconductor 3.19 (R 4.4.0)
alabaster.schemas	1.4.0		Bioconductor 3.19 (R 4.4.0)
alabaster.se	1.4.1		Bioconductor 3.19 (R 4.4.1)
apcluster	1.4.13		RSPM (R 4.4.0)
ape	5.8		CRAN (R 4.4.0)
aplot	0.2.3		RSPM (R 4.4.1)
askpass	1.2.1		RSPM (R 4.4.1)
assertthat	0.2.1		CRAN (R 4.4.0)
babelgene	22.9		RSPM (R 4.4.0)
backports	1.5.0		RSPM (R 4.4.0)
base64enc	0.1-3		CRAN (R 4.4.0)
base64url	1.4		RSPM (R 4.4.0)
batchelor	1.20.0		Bioconductor 3.19 (R 4.4.0)
beachmat	2.20.0		Bioconductor 3.19 (R 4.4.0)
beeswarm	0.4.0		CRAN (R 4.4.0)

package	loaded	version	source
bib2df	1.1.2.0	Github (ropen-sci/bib2df@de0838da561544361d9be6ff20192d0d1c794cde)	
biomaRt	2.60.1	Bioconductor 3.19 (R 4.4.1)	
bit	4.5.0	RSPM (R 4.4.1)	
bit64	4.5.2	RSPM (R 4.4.1)	
bitops	1.0-9	RSPM (R 4.4.1)	
blob	1.2.4	CRAN (R 4.4.0)	
bluster	1.14.0	Bioconductor 3.19 (R 4.4.0)	
boot	1.3-31	CRAN (R 4.4.2)	
broom	1.0.7	RSPM (R 4.4.1)	
bslib	0.8.0	CRAN (R 4.4.1)	
cachem	1.1.0	CRAN (R 4.4.0)	
callr	3.7.6	CRAN (R 4.4.0)	
car	3.1-3	CRAN (R 4.4.1)	
carData	3.0-5	CRAN (R 4.4.0)	
cellity	1.32.0	Bioconductor 3.19 (R 4.4.0)	
cellranger	1.1.0	CRAN (R 4.4.0)	
circlize	0.4.16	CRAN (R 4.4.0)	
class	7.3-23	CRAN (R 4.4.2)	
cli	3.6.3	RSPM (R 4.4.1)	
clue	0.3-66	CRAN (R 4.4.2)	
cluster	2.1.8	CRAN (R 4.4.2)	
clusterProfiler	4.12.6	Bioconductor 3.19 (R 4.4.1)	
coda	0.19-4.1	RSPM (R 4.4.0)	
codetools	0.2-19	CRAN (R 4.2.2)	

package	loaded	version	source
colorspace	2.1-1	RSPM (R 4.4.1)	
corrgram	1.14	CRAN (R 4.4.0)	
cowplot	1.1.3	CRAN (R 4.4.0)	
crayon	1.5.3	RSPM (R 4.4.1)	
crosstalk	1.2.1	CRAN (R 4.4.0)	
curl	6.0.0	RSPM (R 4.4.2)	
data.table	1.16.2	RSPM (R 4.4.1)	
dbplyr	2.5.0	CRAN (R 4.4.0)	
deldir	2.0-4	CRAN (R 4.4.0)	
dichromat	2.0-0.1	CRAN (R 4.4.0)	
digest	0.6.37	CRAN (R 4.4.1)	
doParallel	1.0.17	CRAN (R 4.4.0)	
doRNG	1.8.6	CRAN (R 4.4.0)	
dotCall64	1.2	RSPM (R 4.4.1)	
downlit	0.4.4	RSPM (R 4.4.1)	
dplyr	1.1.4	CRAN (R 4.4.0)	
dqrng	0.4.1	RSPM (R 4.4.0)	
e1071	1.7-16	RSPM (R 4.4.1)	
edgeR	4.2.2	Bioconductor 3.19 (R 4.4.1)	
emmeans	1.10.5	RSPM (R 4.4.1)	
english	1.2-6	RSPM (R 4.4.0)	
enrichR	3.2	RSPM (R 4.4.0)	
enrichplot	1.24.4	Bioconductor 3.19 (R 4.4.1)	
ensemblDb	2.28.1	Bioconductor 3.19 (R 4.4.1)	
estimability	1.5.1	RSPM (R 4.4.0)	

package	loaded	version	source
europepmc	0.4.3	CRAN (R 4.4.0)	
evaluate	1.0.1	RSPM (R 4.4.1)	
ewceData	1.12.0	Bioconductor 3.19 (R 4.4.0)	
fansi	1.0.6	CRAN (R 4.4.0)	
farver	2.1.2	CRAN (R 4.4.0)	
fastDummies	1.7.4	RSPM (R 4.4.1)	
fastmap	1.2.0	RSPM (R 4.4.0)	
fastmatch	1.1-4	CRAN (R 4.4.0)	
fftw	1.0-9	RSPM (R 4.4.1)	
fgsea	1.30.0	Bioconductor 3.19 (R 4.4.0)	
filelock	1.0.3	CRAN (R 4.4.0)	
fitdistrplus	1.2-1	RSPM (R 4.4.1)	
forcats	1.0.0	CRAN (R 4.4.0)	
foreach	1.5.2	CRAN (R 4.4.0)	
formattable	0.2.1	RSPM (R 4.4.0)	
fs	1.6.5	RSPM (R 4.4.2)	
furrr	0.3.1	CRAN (R 4.4.0)	
future	1.34.0	CRAN (R 4.4.1)	
future.apply	1.11.3	RSPM (R 4.4.2)	
gage	2.54.0	Bioconductor 3.19 (R 4.4.0)	
gageData	2.42.0	Bioconductor 3.19 (R 4.4.0)	
gargle	1.5.2	CRAN (R 4.4.0)	
generics	0.1.3	CRAN (R 4.4.0)	
ggalluvial	0.12.5	CRAN (R 4.4.0)	
ggbeeswarm	0.7.2	CRAN (R 4.4.0)	

package	loaded	version	source
ggdendro	0.2.0	RSPM (R 4.4.0)	
ggforce	0.4.2	CRAN (R 4.4.0)	
ggfun	0.1.7	RSPM (R 4.4.2)	
gnetwork	0.5.13	RSPM (R 4.4.0)	
ggplot2	3.5.1	CRAN (R 4.4.0)	
ggplotify	0.1.2	CRAN (R 4.4.0)	
ggbpbr	0.6.0	CRAN (R 4.4.0)	
ggraph	2.2.1	CRAN (R 4.4.0)	
ggrepel	0.9.6	RSPM (R 4.4.1)	
ggridges	0.5.6	CRAN (R 4.4.0)	
ggsci	3.2.0	RSPM (R 4.4.1)	
ggsignif	0.6.4	CRAN (R 4.4.0)	
ggtree	3.12.0	Bioconductor 3.19 (R 4.4.0)	
ggvenn	0.1.10	CRAN (R 4.4.0)	
globals	0.16.3	CRAN (R 4.4.0)	
glue	1.8.0	RSPM (R 4.4.1)	
goftest	1.2-3	CRAN (R 4.4.0)	
googleAuthR	2.0.2	RSPM (R 4.4.0)	
gprofiler2	0.2.3	RSPM (R 4.4.0)	
graph	1.82.0	Bioconductor 3.19 (R 4.4.0)	
graphlayouts	1.2.0	RSPM (R 4.4.1)	
gridBase	0.4-7	CRAN (R 4.4.0)	
gridExtra	2.3	CRAN (R 4.4.0)	
gridGraphics	0.5-1	CRAN (R 4.4.0)	
grr	0.9.5	RSPM (R 4.4.0)	

package	loaded	version	source
gson		0.1.0	CRAN (R 4.4.0)
gt		0.11.1	RSPM (R 4.4.1)
gttable		0.3.6	RSPM (R 4.4.2)
gypsum		1.0.1	Bioconductor 3.19 (R 4.4.0)
haven		2.5.4	CRAN (R 4.4.0)
here		1.0.1	CRAN (R 4.4.0)
hms		1.1.3	CRAN (R 4.4.0)
homologene		1.4.68.19.3.2	RSPM (R 4.4.0)
htmltools		0.5.8.1	CRAN (R 4.4.0)
htmlwidgets		1.6.4	CRAN (R 4.4.0)
httpuv		1.6.15	CRAN (R 4.4.0)
httr		1.4.7	CRAN (R 4.4.0)
httr2		1.0.6	RSPM (R 4.4.2)
humaniformat		0.6.0	RSPM (R 4.4.0)
ica		1.0-3	CRAN (R 4.4.0)
igraph		2.1.1	RSPM (R 4.4.1)
irlba		2.3.5.1	CRAN (R 4.4.0)
iterators		1.0.14	CRAN (R 4.4.0)
janeaustenr		1.0.0	CRAN (R 4.4.0)
janitor		2.2.0	CRAN (R 4.4.0)
jquerylib		0.1.4	CRAN (R 4.4.0)
jsonlite		1.8.9	RSPM (R 4.4.1)
kBET		0.99.6	Github (theislab/k-BET@afc5f431bcbe7d73267acc066a0f2e4eaa10a355)
kableExtra		1.4.0	CRAN (R 4.4.0)

package	loaded	version	source
knitr	1.49	RSPM (R 4.4.2)	
labelled	2.13.0	CRAN (R 4.4.0)	
later	1.3.2	CRAN (R 4.4.0)	
lattice	0.22-5	CRAN (R 4.3.1)	
lazyeval	0.2.2	CRAN (R 4.4.0)	
leaflet	2.2.2	RSPM (R 4.4.0)	
leiden	0.4.3.1	CRAN (R 4.4.0)	
lifecycle	1.0.4	CRAN (R 4.4.0)	
limma	3.60.6	Bioconductor 3.19 (R 4.4.1)	
listenv	0.9.1	CRAN (R 4.4.0)	
lme4	1.1-35.5	RSPM (R 4.4.2)	
lmtest	0.9-40	CRAN (R 4.4.0)	
locfit	1.5-9.10	RSPM (R 4.4.1)	
lubridate	1.9.3	CRAN (R 4.4.0)	
magrittr	2.0.3	CRAN (R 4.4.0)	
mapproj	1.2.11	CRAN (R 4.4.0)	
maps	3.4.2.1	RSPM (R 4.4.2)	
matrixStats	1.4.1	RSPM (R 4.4.1)	
maxLik	1.5-2.1	RSPM (R 4.4.0)	
memoise	2.0.1	CRAN (R 4.4.0)	
metapod	1.12.0	Bioconductor 3.19 (R 4.4.0)	
mime	0.12	CRAN (R 4.4.0)	
miniUI	0.1.1.1	CRAN (R 4.4.0)	
minqa	1.2.8	RSPM (R 4.4.1)	
miscTools	0.6-28	RSPM (R 4.4.0)	

package	loaded	version	source
monocle3	1.3.7		Github (cole-trapnell-lab/monocle3@98402ed0c10cac020524bebbb9300614a799f6d1)
munsell	0.5.1		CRAN (R 4.4.0)
mvoutlier	2.1.1		CRAN (R 4.4.0)
mvtnorm	1.3-2		RSPM (R 4.4.2)
network	1.18.2		RSPM (R 4.4.0)
nlme	3.1-167		CRAN (R 4.4.2)
nloptr	2.1.1		RSPM (R 4.4.1)
openssl	2.2.2		RSPM (R 4.4.1)
org.Hs.eg.db	3.19.1		Bioconductor
org.Mm.eg.db	3.19.1		Bioconductor
orthogene	1.10.0		Bioconductor 3.19 (R 4.4.0)
paletteer	1.6.0		RSPM (R 4.4.0)
pals	1.9		RSPM (R 4.4.1)
parallelly	1.39.0		RSPM (R 4.4.2)
patchwork	1.3.0		RSPM (R 4.4.1)
pathview	1.44.0		Bioconductor 3.19 (R 4.4.0)
pbapply	1.7-2		CRAN (R 4.4.0)
pcaPP	2.0-5		CRAN (R 4.4.1)
pheatmap	1.0.12		CRAN (R 4.4.0)
pillar	1.9.0		CRAN (R 4.4.0)
pkgconfig	2.0.3		CRAN (R 4.4.0)
plotly	4.10.4.9000		Github (ropensci/plotly@cc49ee5db384bdd927b57241b40bf05cdca45438)
plyr	1.8.9		CRAN (R 4.4.0)

package	loaded	version	source
png	0.1-8		CRAN (R 4.4.0)
polyclip	1.10-7		RSPM (R 4.4.1)
preprocessCore	1.66.0		Bioconductor 3.19 (R 4.4.0)
presto	1.0.0		Github (immunogenomic- s/presto@7636b3d0465c468c35853f82f1717d3a64b3c8f6)
prettyunits	1.2.0		CRAN (R 4.4.0)
processx	3.8.4		CRAN (R 4.4.0)
progress	1.2.3		CRAN (R 4.4.0)
progressr	0.15.0		RSPM (R 4.4.2)
promises	1.3.0		CRAN (R 4.4.0)
proxy	0.4-27		CRAN (R 4.4.0)
ps	1.8.1		RSPM (R 4.4.2)
purrr	1.0.2		CRAN (R 4.4.0)
qs	0.27.2		RSPM (R 4.4.1)
qusage	2.38.0		Bioconductor 3.19 (R 4.4.0)
qvalue	2.36.0		Bioconductor 3.19 (R 4.4.0)
rappdirs	0.3.3		CRAN (R 4.4.0)
readr	2.1.5		CRAN (R 4.4.0)
readxl	1.4.3		CRAN (R 4.4.0)
registry	0.5-1		CRAN (R 4.4.0)
rematch2	2.1.2		CRAN (R 4.4.0)
remotes	2.5.0		CRAN (R 4.4.0)
reshape	0.8.9		CRAN (R 4.4.0)
reshape2	1.4.4		CRAN (R 4.4.0)
restfulr	0.0.15		CRAN (R 4.4.0)

package	loaded	version	source
reticulate		1.39.0	RSPM (R 4.4.1)
r hdf5		2.48.0	Bioconductor 3.19 (R 4.4.0)
r hdf5filters		1.16.0	Bioconductor 3.19 (R 4.4.0)
r json		0.2.23	RSPM (R 4.4.1)
r lang		1.1.4	RSPM (R 4.4.1)
r liger		2.1.0	RSPM (R 4.4.2)
r markdown		2.29	RSPM (R 4.4.2)
r ngt tools		1.5.2	CRAN (R 4.4.0)
r robustbase		0.99-4-1	RSPM (R 4.4.1)
r projroot		2.0.4	CRAN (R 4.4.0)
r rcov		1.7-6	CRAN (R 4.4.1)
r rv go		1.16.0	Bioconductor 3.19 (R 4.4.0)
r statix		0.7.2	CRAN (R 4.4.0)
r studioapi		0.17.1	CRAN (R 4.4.1)
r svd		1.0.5	CRAN (R 4.4.0)
r tracklayer		1.64.0	Bioconductor 3.19 (R 4.4.0)
sandwich		3.1-1	RSPM (R 4.4.1)
sass		0.4.9	CRAN (R 4.4.0)
scFlow		0.7.4	Github (neurogenomic-s/scFlow@065bc13dacee707a0437fb65e006647660fc13c7)
scProportionTest		0.0.0.9000	Github (rpolicastro/scProportion-Test@37a04900be1c991428da15af7f9aa7b0ad84661e)
scRNAseq		2.18.0	Bioconductor 3.19 (R 4.4.0)
scales		1.3.0	CRAN (R 4.4.0)
scater		1.32.1	Bioconductor 3.19 (R 4.4.1)

package	loaded	version	source
scattermore	1.2		CRAN (R 4.4.0)
scatterpie	0.2.4		RSPM (R 4.4.1)
scatterplot3d	0.3-44		CRAN (R 4.4.0)
scran	1.32.0		Bioconductor 3.19 (R 4.4.0)
sctransform	0.4.1		CRAN (R 4.4.0)
scuttle	1.14.0		Bioconductor 3.19 (R 4.4.0)
secretbase	1.0.3		RSPM (R 4.4.1)
sessioninfo	1.2.2		RSPM (R 4.4.0)
sgeostat	1.0-27		CRAN (R 4.4.0)
shadowtext	0.1.4		RSPM (R 4.4.1)
shape	1.4.6.1		CRAN (R 4.4.0)
shiny	1.9.1		RSPM (R 4.4.1)
simona	1.2.0		Bioconductor 3.19 (R 4.4.0)
slam	0.1-55		CRAN (R 4.4.2)
sna	2.8		RSPM (R 4.4.1)
snakecase	0.11.1		CRAN (R 4.4.0)
sp	2.1-4		CRAN (R 4.4.0)
spam	2.11-0		RSPM (R 4.4.1)
sparseMatrixStats	1.16.0		Bioconductor 3.19 (R 4.4.0)
spatstat.data	3.1-2		RSPM (R 4.4.1)
spatstat.explore	3.3-3		CRAN (R 4.4.1)
spatstat.geom	3.3-3		RSPM (R 4.4.1)
spatstat.random	3.3-2		RSPM (R 4.4.1)
spatstat.sparse	3.1-0		RSPM (R 4.4.1)
spatstat.univar	3.1-1		RSPM (R 4.4.2)

package	loaded	version	source
spatstat.utils	3.1-1	RSPM (R 4.4.2)	
speckle	1.4.0	Bioconductor 3.19 (R 4.4.0)	
splitstackshape	1.4.8	RSPM (R 4.4.0)	
statmod	1.5.0	CRAN (R 4.4.0)	
statnet.common	4.10.0	RSPM (R 4.4.1)	
stringfish	0.16.0	RSPM (R 4.4.0)	
stringi	1.8.4	RSPM (R 4.4.0)	
stringr	1.5.1	CRAN (R 4.4.0)	
survival	3.8-3	CRAN (R 4.4.2)	
svglite	2.1.3	CRAN (R 4.4.0)	
systemfonts	1.1.0	RSPM (R 4.4.0)	
targets	1.8.0	RSPM (R 4.4.1)	
tensor	1.5	CRAN (R 4.4.0)	
threejs	0.3.3	RSPM (R 4.4.0)	
tibble	3.2.1	CRAN (R 4.4.0)	
tidygraph	1.3.1	CRAN (R 4.4.0)	
tidyrr	1.3.1	CRAN (R 4.4.0)	
tidyselect	1.2.1	CRAN (R 4.4.0)	
tidytext	0.4.2	CRAN (R 4.4.0)	
tidytree	0.4.6	CRAN (R 4.4.0)	
timechange	0.3.0	CRAN (R 4.4.0)	
tm	0.7-14	RSPM (R 4.4.1)	
tokenizers	0.3.0	CRAN (R 4.4.0)	
topGO	2.56.0	Bioconductor 3.19 (R 4.4.0)	
treeio	1.28.0	Bioconductor 3.19 (R 4.4.0)	

package	loaded	version	source
treemap	2.4-4	CRAN (R 4.4.0)	
triebeard	0.4.1	CRAN (R 4.4.0)	
tweenr	2.0.3	CRAN (R 4.4.0)	
tzdb	0.4.0	CRAN (R 4.4.0)	
umap	0.2.10.0	CRAN (R 4.4.0)	
urltools	1.7.3	CRAN (R 4.4.0)	
utf8	1.2.4	CRAN (R 4.4.0)	
uwot	0.2.2	RSPM (R 4.4.0)	
vctrs	0.6.5	CRAN (R 4.4.0)	
vipor	0.4.7	CRAN (R 4.4.0)	
viridis	0.6.5	CRAN (R 4.4.0)	
viridisLite	0.4.2	CRAN (R 4.4.0)	
vroom	1.6.5	CRAN (R 4.4.0)	
wesanderson	0.3.7	CRAN (R 4.4.0)	
whisker	0.4.1	RSPM (R 4.4.0)	
withr	3.0.2	RSPM (R 4.4.2)	
wordcloud	2.6	CRAN (R 4.4.0)	
xfun	0.49	RSPM (R 4.4.2)	
xml2	1.3.6	CRAN (R 4.4.0)	
xtable	1.8-4	CRAN (R 4.4.0)	
yaml	2.3.10	RSPM (R 4.4.1)	
yulab.utils	0.1.8	RSPM (R 4.4.2)	
zlibbioc	1.50.0	Bioconductor 3.19 (R 4.4.0)	
zoo	1.8-12	CRAN (R 4.4.0)	

Figure 1

(A) Neurovascular unit isolation method. (B)

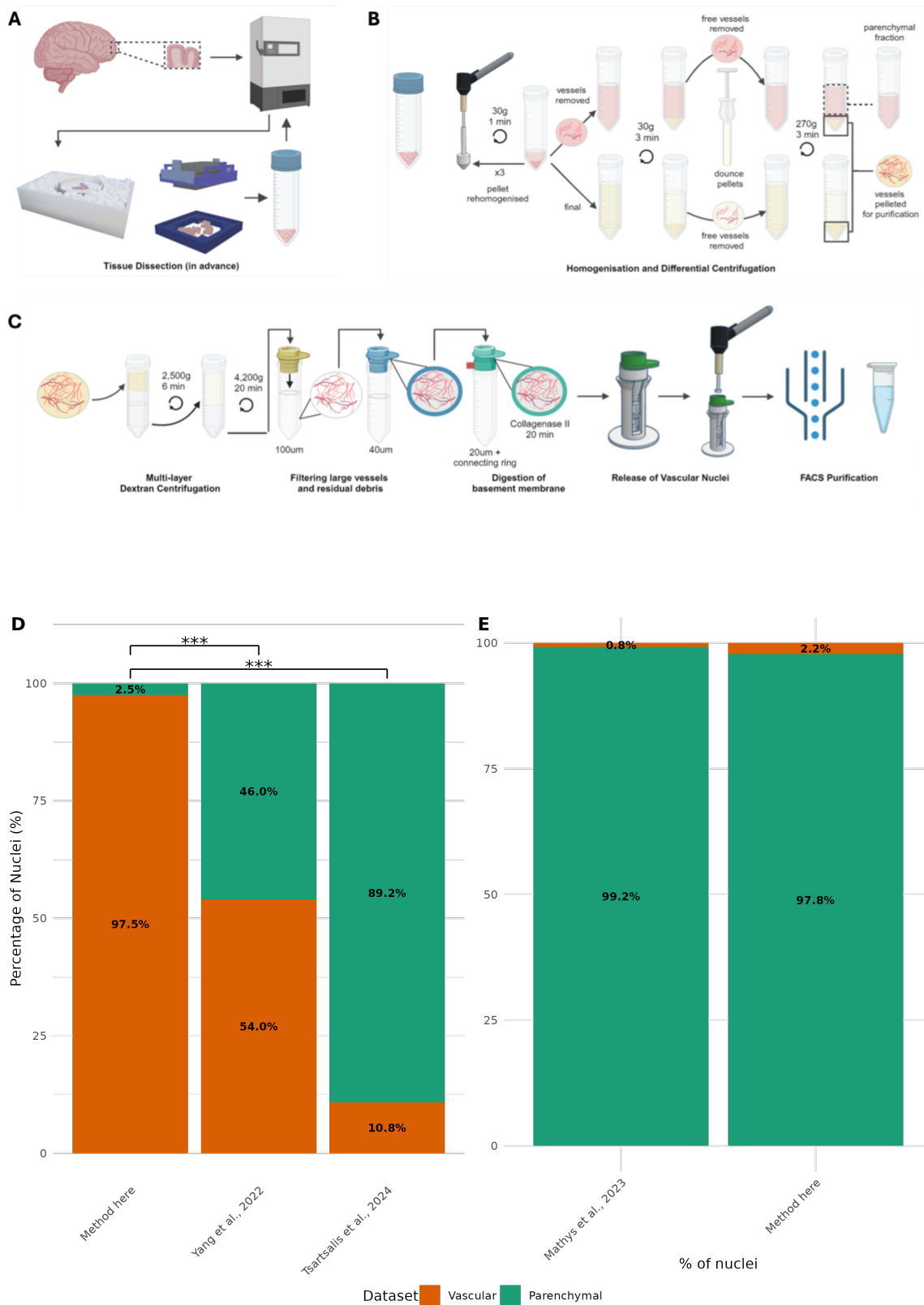


Figure 2

(A) figure legend stuff

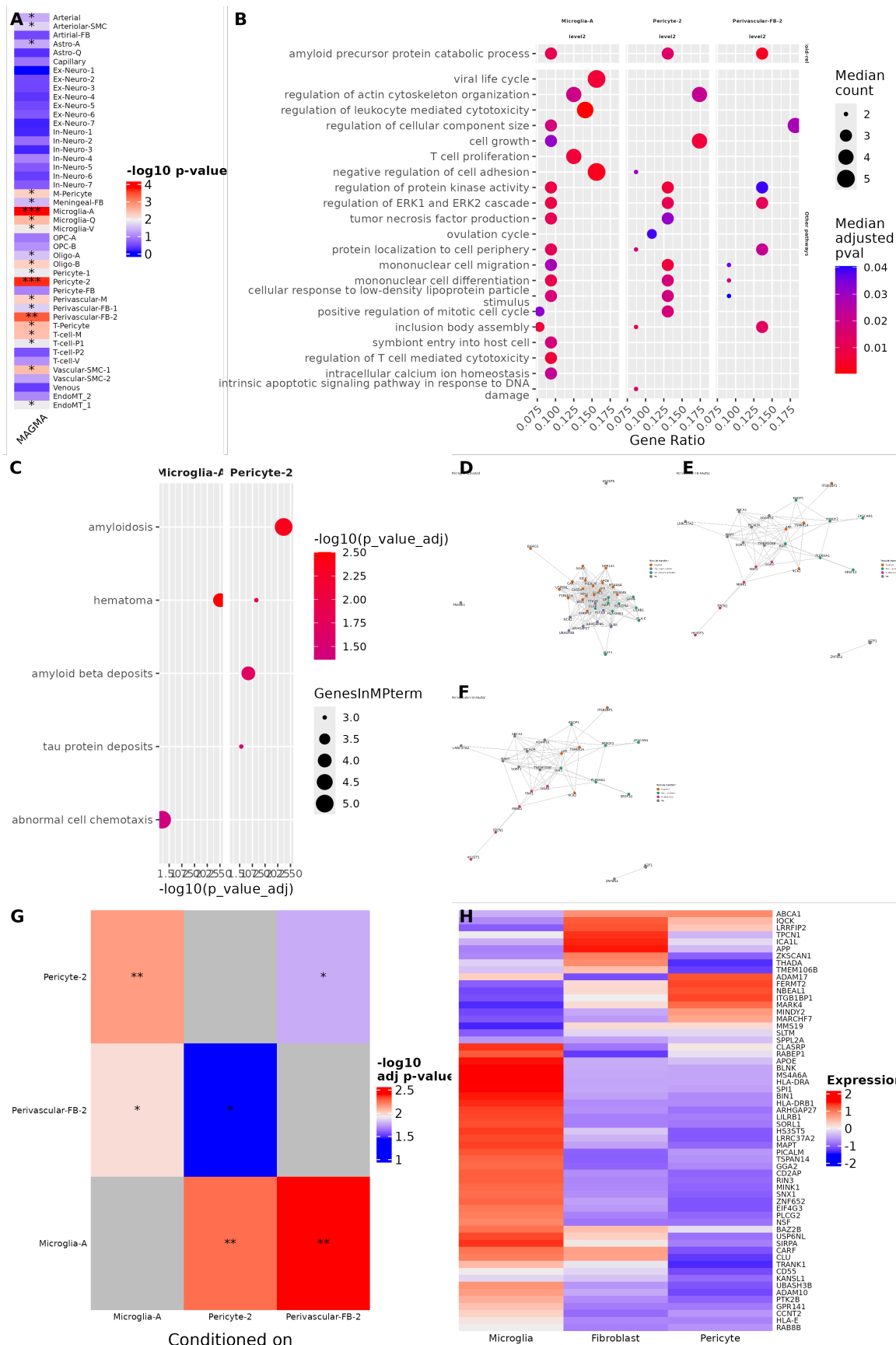


Figure 3

(A) Heatmap of differential number and strength of interactions. (B)

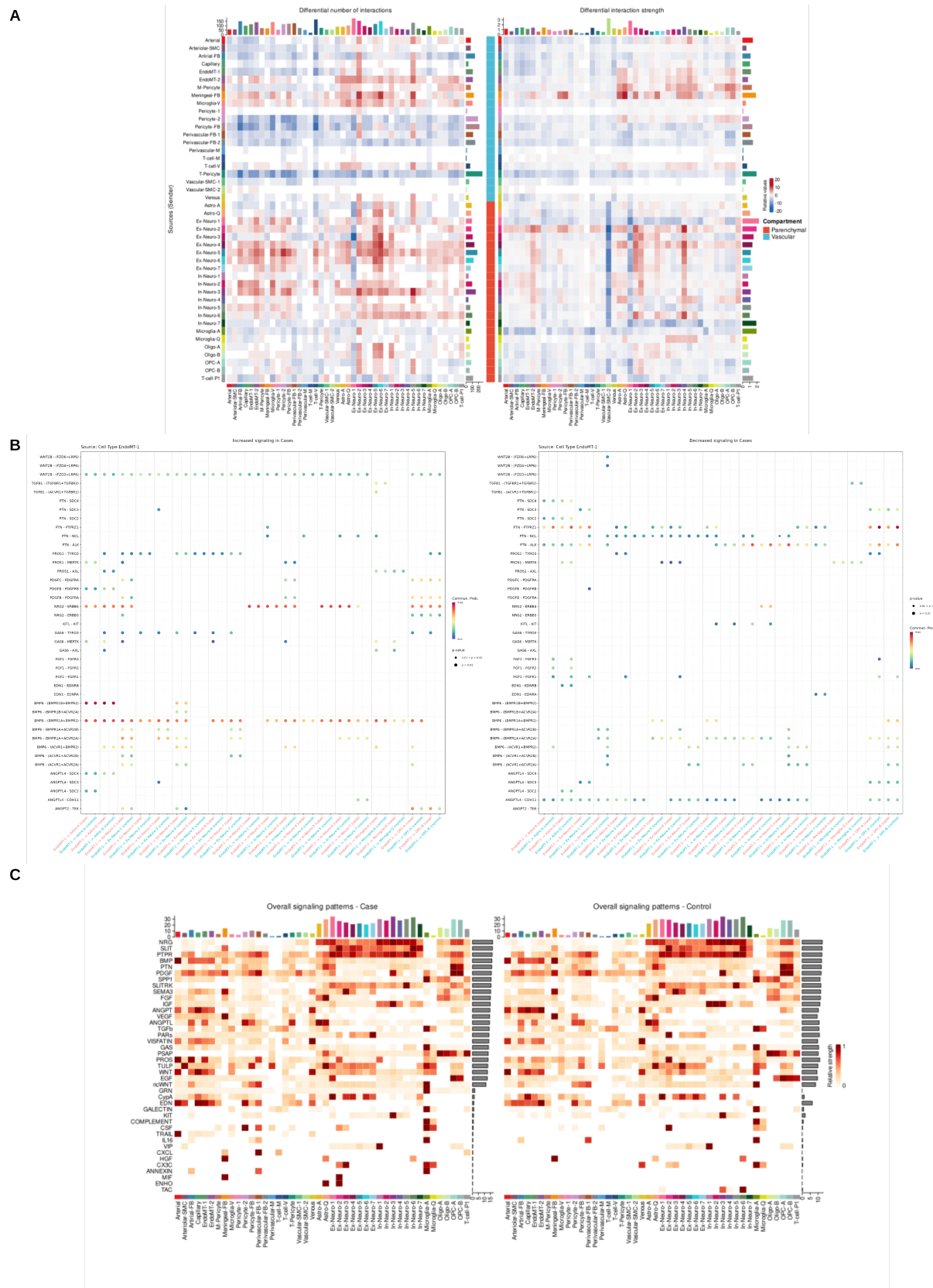


Figure 4

(A) Counts of DEGs. (B)

